Hyperfine Interactions **144/145:** 141–149, 2002.

Influence of the Interfaces on Magnetic Properties of Fe/Ag and Fe/Cu Multilayers Prepared by Sputtering

A. P. KUPRIN*, L. CHENG, Z. ALTOUNIAN and D. H. RYAN
Physics Department and Centre for the Physics of Materials, McGill University, 3600 University Street, Montreal, Quebec H3A 2T8, Canada

Abstract. Dependence of magnetic behavior of ultrathin Fe layers on the width of the interfaces was investigated by using dc-magnetron sputtering to grow (Fe(110)/Ag(111)) multilayers (ML) with thin interfaces and (Fe(111)/Cu(111)) multilayer with wide interfaces. Thicknesses of non-magnetic layers in all cases were 25 Å. The Fe/Ag MLs were prepared with thickness of Fe layers t_{Fe} = 8.8 Å and 2.4 Å, while Cu/Fe ML had the largest t_{Fe} = 11.0 Å together with widest interfaces. In-field ^{57}Fe conversion electron Mössbauer spectroscopy (CEMS) down to 50 K was employed to show that Fe layers are not uniform, to characterize interfaces, and to distinguish between static and relaxation behavior. This allowed unambiguous interpretation of T-dependencies of susceptibility and spontaneous magnetisation upon crossover to island structure of the Fe layers.

Key words: low-temperature conversion electron Mössbauer spectroscopy, magnetic multilayers, interfaces, temperature decay of magnetization.

1. Introduction and methods

Data storage and information transport technologies at present involve magnetic structures with lateral sizes less than a micrometer with a continuing tendency to approach a nanometer scale where high stability to thermal magnetization decay is a key issue. Though magnetism of thin Fe films was extensively studied experimentally, including Mössbauer spectroscopy, in connection with the 3D–2D crossover [1] and a variety of magnetic states of fcc γ-Fe that depend on the atomic volume [2], the finite-size effects associated with a decrease of lateral size of the layers received less attention. In most of the works Fe films were grown epitaxially in UHV that resulted in high monocrystalline quality and practically atomically flat interfaces. Previously, we investigated how significant interface roughness and intermixing in Fe/Cu multilayers prepared by sputtering may result in break up of the layers into isolated islands [3]. As sputtering provides a convenient way to vary the width of the interfaces we used this method to prepare two different kind of multilayers. Two Fe/Ag multilayers were grown to investigate transition

* Present address: Physics Department, University of California, San Diego, 9500 Gilman Drive, La Jolla, CA 92093-0319, USA.

Table I. Structural parameters and growth conditions of Fe/Ag and Fe/Cu multilayers. N is the number of bilayer repetitions, t_{Fe}, t_{nm} are the thicknesses of Fe and non-magnetic elemental layers, $\sigma_{nm/Fe}$ and $\sigma_{Fe/nm}$ are the roughnesses of the interfaces (NM/Fe means Fe on top of non-magnetic metal), P_{Ar} is an Ar pressure during deposition, and R_{nm} and R_{Fe} are the deposition rates

Name	Spacer	N	t_{Fe} (Å)	t_{nm} (Å)	$\sigma_{nm/Fe}$ (Å)	$\sigma_{Fe/nm}$ (Å)	P_{Ar} (mTorr)	R_{nm} (Å/s)	R_{Fe} (Å/s)
ML8.8	Ag	25	8.8	25.3	6.6	13.0	10	3.0	1.0
ML2.4	Ag	25	2.4	28.3	7.7	9.8	10	3.0	1.0
ML11.0	Cu	36	11.0	25.1	12.5	34.0	20	1.9	0.8

to island morphology of the Fe layers in the case when interfaces are sharp due to a strong de-mixing tendency and small band hybridization between Fe and Ag. One Fe/Cu multilayer was also prepared to represent the opposite case of continuous layers with wide interfaces. In all cases, the thickness of non-magnetic layers t_{nm} was much larger than thickness of the Fe layers t_{Fe} to escape interlayer coupling. Fe(110)/Ag(111) and Fe(111)/Cu(111) orientations were found by high-angle XRD. Parameters of the multilayers were determined from fits to small-angle X-ray reflectivity data and are summarized in Table I. The crucial details about magnetic and structural properties on local scale both in remanent state as well as with in-plane external field were obtained by ^{57}Fe low-temperature conversion electron Mössbauer spectroscopy (LT-CEMS) down to 50 K. We built two gas proportional counters based on the prototype designed at Mainz [4] and optimized for low-temperatures in respect of S/N ratio and energy resolution. Important features of the counters are: thin sensitive volume of 3 mm in thickness only (1 mm anode-sample distance) to compensate for increased gas density, spring support for the anode wire to accommodate shrinkage of the dimensions, double mylar windows in the detector's body and its cap with inter-window volume connected to the sensitive volume to keep walls of the sensitive chamber always flat, and electrical isolation of the detector body from the inner parts of the cryostats. Operating voltage was optimized for each working temperature in respect of reducing measurement time [5]. Gas-flow He + 4%CH_4 counter was used in the temperature range 320–90 K inside standard liquid N_2 cryostat, while gas-filled He counter was used down to 50 K in the in-house made cryostat filled with He-gas for heat exchange and cooled by the vibration-isolated closed cycle He refrigerator. Both counters allowed simultaneous acquisition of spectra in backscattering CEMS and transmission geometries, and showed stable long-term operation and proved to be very effective for our thin samples (with natural isotopic content). Magnetic properties in the bulk were characterized by initial susceptibility χ_{ac} measured with the ac excitation field of 70 Hz and amplitude of 5 Oe and by spontaneous magnetization M_s extrapolated to zero field from measurements in the external field of 4 T strong enough to saturate our multilayers at any orientation.

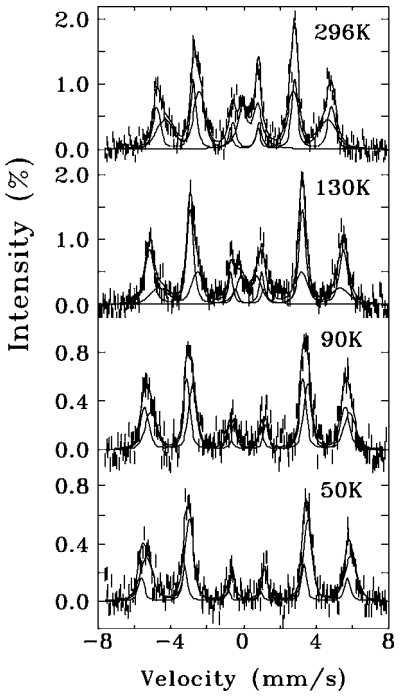

Figure 1. Conversion electron Mössbauer spectra for the (Fe 8.8 Å/Ag 25.3 Å)×25 multilayer in the range 50 K–room temperature. Strong Zeeman splitting persist to RT. Note a weak signal that appears at around zero velocity at the increased temperatures only. Details of decomposition are described in the text.

2. Results

Selected CEMS spectra of the Fe/Ag multilayers ML8.8 and ML2.4 are shown in Figure 1 and Figure 2 respectively. At 50 K spectra represent a ferromagnetic (FM) Zeeman splitting. Asymmetrical broadening of lines suggests at least two components that were modeled by two sextets with symmetrical Gaussian distribution of hyperfine fields (P(B_{hf})) for each of them. This contrasts with MBE-grown multilayers when Fe(110)/Ag(111) orientation exhibits a single sextet only, but two or three sextets are necessary to fit spectra for Fe(100)/Ag(100) orientation and may be ascribed to the different physical nature of deposition processes used. Considering that top and bottom interfaces are distinctly different as reflected in Table I, and similar to the case of sputtered Fe(111)/Cu(111) multilayers [3], it is logical to ascribe the sextet (S_{bi}) with larger average field $\langle B_{\mathrm{hf}}\rangle$ having narrower P(B_{hf}) and smaller isomer shift (we used α-Fe at RT as a reference) to the bottom interface together with the inner regions, and another sextet (S_{t}) to the top interface, following results on site-probed Fe(100)/Ag(100) multilayers ([6] and references therein). Widths of both distributions are much broader for ML2.4, especially for S_{bi} and partial contribution of S_{t} is strongly decreased. Partial contributions of S_{bi}

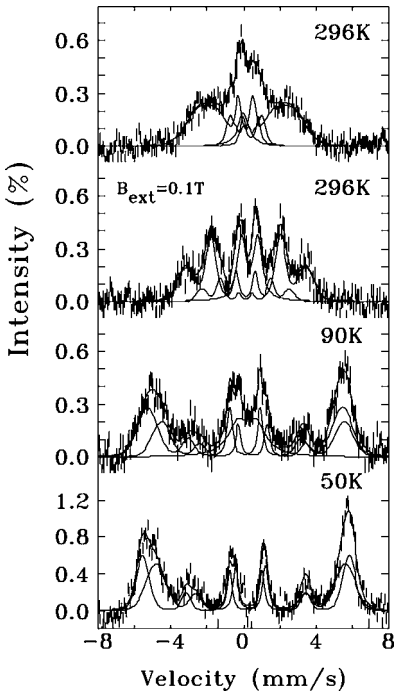

Figure 2. Conversion electron Mössbauer spectra for the (Fe 2.4 Å/Ag 28.3 Å)×25 multilayer in the range 50 K–room temperature. Note that lines are much wider than for the multilayer shown in Figure 1. Zeeman splitting collapses at around room temperature to spin-glass-like pattern. External in-plane magnetic field of 0.1 T increases hyperfine splitting and resolves constituent lines; details are in the text.

and S_t for both samples roughly correspond to the ratio of interface roughnesses in Table I, suggesting that the inner regions of pure Fe are rather small. At 50 K the average field of S_{bi} is essentially the same for both samples $\langle B_{hf}^{bi} \rangle = (35.4 \pm 0.2)$ T, while splitting of S_t is notably less for thinner Fe layers with $\langle B_{hf}^{t} \rangle = (35.0 \pm 0.1)$ T and (32.5 ± 0.3) T for ML8.8 and ML2.4, respectively.

On raising temperature, signal around zero velocity starts to appear pointing to superparamagnetizm of a part of the Fe layers. Its parameters practically do not change with temperature (isomer shift $\delta = +0.2$–0.4 mm/s, quadrupole splitting $\Delta = 0.8$–0.9 mm/s) and are in the range for small Fe clusters in Ag seen previously even in MBE-grown Fe/Ag system [7] and references therein. But its partial contribution to the spectrum increases first at the expense of the S_t, in agreement with expectations of a weaker magnetic interactions in more rough and alloyed top interface. For ML8.8 it is reliably resolved at 130 K and corresponds to a doublet (D). Nevertheless, its partial contribution is relatively small being 17% in the RT spectrum and external in-plane magnetic field $B_{ext} = 0.1$ T does not increase its contribution and results in the identical spectrum. Dominant contribution of the FM signal and completely in-plane alignment of magnetization for both sextets

in the whole temperature range studied shows that the 8.8 Å thick Fe layers are quite uniform and at least several atomic layers (AL) thick on macroscopic scale (1 AL Fe(110) = 2.03 Å) with Curie temperature (T_c) far above RT. For ML2.4 a doublet appears at lower temperatures and constitutes 20% of the signal already at 90 K. Further increase of temperature leads to a dramatic spectral changes, but affects S_t more drastically. At RT as compared to 50 K, $\langle B_{hf}^{bi}\rangle$ drops a little more than twice to (15.3 ± 0.4) T, while $\langle B_{hf}^{t}\rangle$ drops almost six times to (5.6 ± 0.3) T. Also, width of the P(B_{hf}) for S_{bi} increases 2.4 times that makes spectrum look like that of an amorphous Fe spin-glass alloy. In addition, a single line appears at about zero velocity. At the same time, direction of magnetization shows no temperature dependence remaining (33 ± 1)° tilted from the normal. Small in-plane B_{ext} = 0.1 T strongly increases $\langle B_{hf}^{t}\rangle$ to (15.0 ± 0.6) T, effect typical for SP behavior [1]. $\langle B_{hf}^{bi}\rangle$ increases only about 30% to (20.6 ± 0.3) T, but P($\langle B_{hf}^{bi}\rangle$) decreases 1.8 times such that Zeeman lines become nicely resolved. Both of these effects suggest more collinear magnetic structure for S_{bi} considering that 1st near-neighbors contribute around 50% to B_{hf} on ^{57}Fe [8]. For both sextets magnetization now lies totally in-plane and single line component disappears suggesting that SP relaxation is effectively suppressed. Hence, one can estimate that at least 33% of the Fe atoms are SP at RT and already at 320 K most of the Fe atoms are engaged in fluctuations as the spectrum (not shown) exhibits a broad single line at zero velocity with typical long relaxation wings [9].

CEMS spectra of the Fe/Cu multilayer ML11.0 are shown in Figure 3. Lines of the Zeeman pattern are much broader than for Fe/Ag multilayers in agreement with a somewhat better solubility of Fe in Cu. Also the paramagnetic (PM) signal in the central part of the spectrum is still present at the lowest temperature. Main features of the spectral shape and its evolution with temperature follows those of Fe/Cu multilayers studied in our group previously ([3] and references therein). Hence, we used the same model to fit present spectra. Upon warming the thinnest FM parts of the Fe layers become PM that is reflected in population of the strong doublet with smaller splitting at the expense of the Zeeman split component. The latter one is modeled at 50 K by two Gaussian distributions. The one with larger field, $\langle B_{inn}\rangle$ = (32.6 ± 1.4) T represents inner FM regions, while the lower field one, $\langle B_{int}\rangle$ = (17.8 ± 2.0) T, – alloyed Fe-rich FM top interfaces. These fields are smaller than $\langle B_{hf}^{bi}\rangle$ and $\langle B_{hf}^{t}\rangle$, respectively, at each temperature of the experiment. This exposes a weaker magnetic exchange in a more intermixed Fe/Cu system notwithstanding that on average ML11.0 has the thickest Fe layers among samples studied of 5.3 AL (1 AL Fe(110) = 2.07 Å). Also magnetization is (62 ± 5)° tilted from the normal, that is about twice more than for ML2.4 with sharpest interfaces, and points to a weaker perpendicular magnetic anisotropy (PMA) due to less sharp interfaces. As in the Fe/Ag multilayers the bottom interfaces are much sharper, but are strikingly different, remaining PM in the whole T-range studied and are modeled by a quadrupole doublet with larger splitting. Its partial contribution to the spectrum is around 10% and independent of temperature. Disappearance of

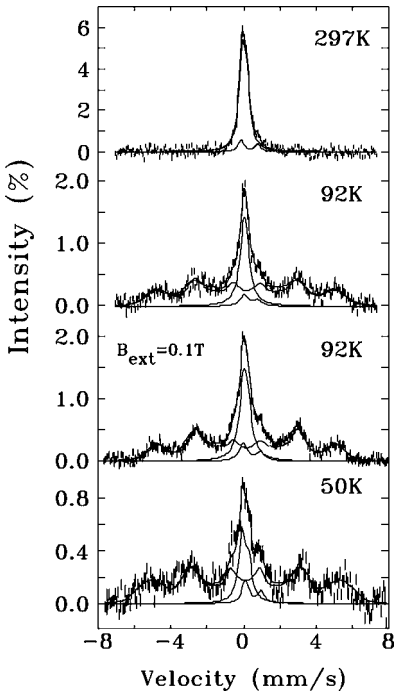

Figure 3. Conversion electron Mössbauer spectra for the (Fe 11.0 Å/Cu 25.0 Å)×36 multilayer in the range 50 K–room temperature. Wide distribution of hyperfine fields is present at low temperatures, which completely collapses on warming before reaching room temperature. External in-plane magnetic field of 0.1 T does not increase hyperfine splitting.

FM contribution happens at $T_c = 250$ K, that is lower than for Fe/Ag multilayers. In-plane $B_{ext} = 0.1$ T applied in the range 90–180 K does not change either visible Zeeman splitting or any of the parameters of the model except orientation of magnetization, rotating it completely into the plane of the multilayer. This shows the absence of any SP relaxation.

Measurements of susceptibility complement ^{57}Fe Mössbauer spectroscopy due to sensitivity not only to critical phenomena and magnetic orientation, but also to domain formation and motion [10] and due to a five orders of magnitude larger characteristic time scale. For ML8.8 film a steady increase of $\chi_{\|}$ on warming from 5 K to a very large value without saturation at RT presented in Figure 4 in principal agrees with conclusion of T_c to be much higher RT obtained from Mössbauer data. And the absence of any pronounced features may be explained by the smearing effect of small but measurable SP islands with large size distribution (due to finite roughness of the interfaces) also seen to be present in Mössbauer spectra. SP behavior is much stronger in ML2.4 due to smaller sizes of isolated Fe islands expected for thinner layers with the blocking temperature (T_B) estimated from Mössbauer data to be slightly above RT. Now $\chi_{\|}$ shows a pronounced hump at a temperature around 150 K, i.e., about twice lower than T_B, situation similar for

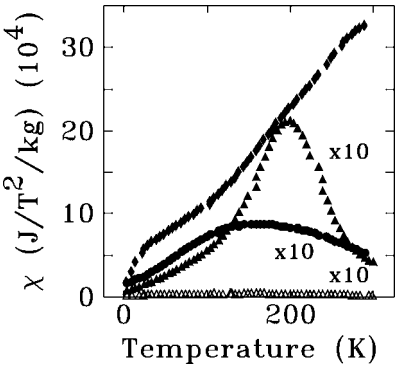

Figure 4. Temperature dependence of the real part of the initial susceptibility: diamonds – for the (Fe 8.8 Å/Ag 25.3 Å)×25 multilayer, circles – for the (Fe 2.4 Å/Ag 28.3 Å)×25 multilayer, triangles – for the (Fe 11.0 Å/Cu 25.1 Å)×36 multilayer. Filled symbols represent susceptibility measured with in-plane excitation field, $\chi_{\parallel}$, open – measured in perpendicular orientation, $\chi_{\perp}$.

nm-size α-Fe particles [9], except for a much broader width of the hump for our sample due to large size distribution of the Fe islands expected for thin sputtered layers. This broad hump cannot be due to formation and motion of domains as no spin-reorientation is detected at these temperatures in Mössbauer spectra [10]. ML11.0 also exhibits a similarly strong signal in $\chi_{\parallel}$ below T_c. But its several times smaller width immediately suggests another explanation than SP relaxation as this multilayer has the roughest interfaces that would result in the largest size-distribution of the Fe islands. Support for the rejection of SP behavior obtained from Mössbauer data comes from T-dependence of $\chi_{\perp}$ that shows no features at all. We note that with excitation the field oriented perpendicular to the film and almost in-plane magnetization at 50 K $\chi_{\perp}$ is insensitive to order–disorder transition and formation of perpendicular domains is excluded [10]. Thus, the peak in $\chi_{\parallel}$ is attributed to the in-plane rotational response of magnetization.

One of the important parameters for practical applications is thermal decay of spontaneous magnetisation, M_s. At low temperatures this process is governed by thermal excitations of spin waves and experimental data in most of the works are fit to a power law [11]. The crossover from 3D to 2D behavior is marked by the change in the exponent from $n = 3/2$ (Bloch-like) to $n = 1$ (quasi-linear) if the energy gap at zero wave vector, whose origin is magnetic anisotropy, is not vanishingly small [12]. For high-quality Fe(110) thin films this happens at thickness around 3 AL [1]. M_s for ML8.8 decreases with temperature most slowly but clearly non-linearly as shown in Figure 5. The fitted to $T^{3/2}$-law spin-wave parameter $B_{\parallel} = (4.3 \pm 0.8)\ 10^{-5}\ K^{-3/2}$ is 5.4 times larger than for the similar multilayer grown by MBE [1]. This agrees with the more strongly reduced exchange coupling expected inside interface areas in sputtered films [13]. For ML2.4 $B_{\parallel}$ experiences an additional increase of 2.0. Though remanent magnetization has a substantial normal component detected in Mössbauer spectra (Figure 2), this does

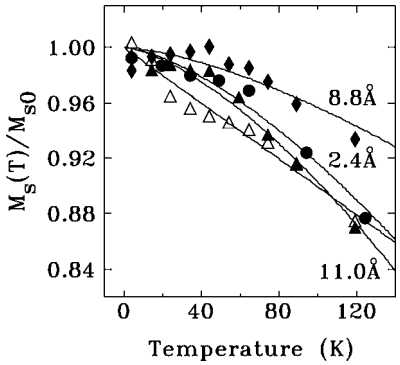

Figure 5. Temperature dependence of reduced spontaneous magnetization obtained from extrapolation of the in-field data up to 4 T to zero field for the (Fe 8.8 Å/Ag 25.3 Å)×25 multilayer (diamonds), (Fe 2.4 Å/Ag 28.3 Å)×25 multilayer (circles), (Fe 11.0 Å/Cu 25.0 Å)×36 multilayer (triangles). Filled symbols represent measurements with the in-plane field, open – in perpendicular orientation.

not necessarily imply that interface magnetic anisotropy became stronger than for ML8.8 as it may prevail merely due to weaker dipolar shape anisotropy as 1–2 AL thick Fe layers are unavoidably broken up into isolated SP patches. This is in contrast with clearly linear M_svT for sputtered Fe(111)/Cu(111) multilayer with discontinuous Fe layers [3] and may be explained by a stronger interlayer coupling in this system that results in a stronger PMA as there are 6 NN in the adjacent atomic planes for Fe(111) orientation, while only 2 NN for Fe(110), even when Fe is more susceptible to intermixing with Cu than Ag. Excessively wide interfaces of ML11.0 should strongly decrease both PMA and in-plane shape anisotropy thus suppressing linear dependence of M_svT. In fact, the decrease of M_s is the fastest with $B_{\parallel} = (9.7 \pm 0.6)\ 10^{-5}\ \mathrm{K}^{-3/2}$ as illustrated in Figure 5. Interestingly, M_svT measured in perpendicular orientation cannot be fitted with $T^{3/2}$-law, contrary to linear fit that gives $B_{\perp} = (101 \pm 7)\ 10^{-5}\ \mathrm{K}^{-1}$. In this orientation external field is applied at a very large angle to the remanent magnetization and should decouple the very outer regions of the Fe layers with small numbers of Fe NN from more uniform inner ones, thus effectively thinning and driving them into 2D regime.

3. Conclusions

Sputtering allows preparation of ultrathin Fe layers with either narrow interfaces or wide and alloyed interfaces. In both Fe/Ag and Fe/Cu multilayers top and bottom interfaces are distinctly different. Top interfaces are much wider and are ferromagnetic in both systems. Bottom interfaces are less alloyed, they are ferromagnetic in Fe/Ag multilayers, but non-magnetic in Fe/Cu multilayers. Widening of the interfaces suppresses perpendicular magnetic anisotropy, drastically increases the decay rate of spontaneous magnetization with temperature, and induces crossover from 3D to 2D magnetism by aligning magnetization normal to the easy plane.

Acknowledgements

This work was supported by grants from the Natural Sciences and Engineering Research Council of Canada and Fonds pour la formation de chercheurs et l'aide à la recherche, Québec.

References

1. Gutierrez, C. J., Qiu, Z. Q., Tang, H., Wieczorek, M. D., Mayer, S. H. and Walker, J. C., *Phys. Rev. B.* **44** (1991), 2190.
2. Keune, W., Schatz, A., Ellerbrock, R. D., Fuest, A., Wilmers, K. and Brand, R. A., *J. Appl. Phys.* **79** (1996), 4265.
3. Kuprin, A. P., Hanžel, D., Ensling, J., Spiering, H. and Gütlich, P., unpublished.
4. Kuprin, A. P. and Novakova, A. A., *Nucl. Instr. Meth. B* **62** (1992), 493.
5. Kuprin, A. P., Cheng, L., Altounian, Z. and Ryan, D. H., *J. Appl. Phys.* **87** (2000), 6591.
6. Keavney, D. J., Wieczorek, M. D., Storm, D. F. and Walker, J. C., *J. Magn. Magn. Mater.* **121** (1993), 49.
7. Kuprin, A., Wiarda, D. and Ryan, D. H., *Phys. Rev. B* **61** (2000), 1267.
8. Volkening, F. A., Jonker, B. T., Krebs, J. J., Koon, N. C. and Prinz, G. A., *J. Appl. Phys.* **63** (1988), 3869.
9. Bødker, F., Mørup, S., Pedersen, M. S., Svedlindh, P., Jonsson, G. T., Garcia-Palacios, J. L. and Lazaro, F. J., *J. Magn. Magn. Mater.* **177–181** (1998), 925.
10. Arnold, C. S., Johnston, H. L. and Venus, D., *Phys. Rev. B* **56** (1997), 8169.
11. Bayreuther, G., *Hyp. Interact.* **47** (1989), 237.
12. Erickson, R. P. and Mills, D. L., *Phys. Rev. B* **44** (1991), 11825.
13. Mathon, J. and Ahmad, S. B., *Phys. Rev. Lett.* **37** (1988), 660.